

SCIENTIFIC REPORTS



OPEN

Ammonium sorption and ammonia inhibition of nitrite-oxidizing bacteria explain contrasting soil N₂O production

Received: 09 April 2015

Accepted: 22 June 2015

Published: 16 July 2015

Rodney T. Venterea^{1,2}, Timothy J. Clough³, Jeffrey A. Coulter⁴, Florence Breuillin-Sessoms⁵ Ping Wang² & Michael J. Sadowsky²

Better understanding of process controls over nitrous oxide (N₂O) production in urine-impacted 'hot spots' and fertilizer bands is needed to improve mitigation strategies and emission models. Following amendment with bovine (*Bos taurus*) urine (Bu) or urea (Ur), we measured inorganic N, pH, N₂O, and genes associated with nitrification in two soils ('L' and 'W') having similar texture, pH, C, and C/N ratio. Solution-phase ammonia (sNH₃) was also calculated accounting for non-linear ammonium (NH₄⁺) sorption capacities (ASC). Soil W displayed greater nitrification rates and nitrate (NO₃⁻) levels than soil L, but was more resistant to nitrite (NO₂⁻) accumulation and produced two to ten times less N₂O than soil L. Genes associated with NO₂⁻ oxidation (*nxrA*) increased substantially in soil W but remained static in soil L. Soil NO₂⁻ was strongly correlated with N₂O production, and cumulative (c-) sNH₃ explained 87% of the variance in c-NO₂⁻. Differences between soils were explained by greater sNH₃ in soil L which inhibited NO₂⁻ oxidation leading to greater NO₂⁻ levels and N₂O production. This is the first study to correlate the dynamics of soil sNH₃, NO₂⁻, N₂O and nitrifier genes, and the first to show how ASC can regulate NO₂⁻ levels and N₂O production.

Better understanding of biochemical process controls over soil N₂O production is needed for improving N₂O mitigation strategies and emissions models. Incorporation of improved process-related information into models will help improve emissions assessments at field, regional and global scales^{1,2}. In cattle grazing systems, urine deposition events typically result in localized N loads equivalent to 1000 kg N ha^{-1,3}, and can create 'hot spots' for elevated N₂O emissions⁴. Similarly, N fertilizers applied in concentrated bands result in localized inorganic N concentrations ranging from several hundred to more than 2000 μg N g^{-1,5,6}, and can result in substantially greater N₂O emissions compared to uniformly applied fertilizer⁷⁻⁹. Thus, understanding the processes mediating N₂O production within these concentrated zones is critical. Urine deposition and Ur application can cause elevated soil NO₂⁻ levels which in turn promote elevated N₂O production⁹⁻¹¹. Accumulation of NO₂⁻ is presumed to occur due to a sequence of chemical and microbial responses. Hydrolysis of Ur results in localized increases in both soil pH and NH₄⁺ which together promote the formation of free NH₃¹². Both groups of autotrophic nitrifying bacteria, i.e., the NH₃-oxidizing bacteria (AOB) and the NO₂⁻ oxidizing bacteria (NOB), are sensitive to NH₃ toxicity, but it is generally believed that NOB are more sensitive than AOB¹¹⁻¹⁴; thus, soil NO₂⁻ accumulates in

¹USDA-ARS, Soil and Water Management Research Unit, St. Paul, MN 55108, USA. ²Dep. of Soil, Water, and Climate, Univ. of Minnesota, St. Paul, MN 55108, USA. ³Faculty of Agriculture and Life Science, Lincoln Univ., PO Box 85084, Lincoln 7647, Canterbury, New Zealand. ⁴Dep. of Agronomy and Plant Genetics, Univ. of Minnesota, St. Paul, MN 55108, USA. ⁵Biotechnology Institute, College of Biological Sciences, Univ. of Minnesota, St. Paul, MN 55108, USA. Correspondence and requests for materials should be addressed to R.V. (email: Venterea@umn.edu)

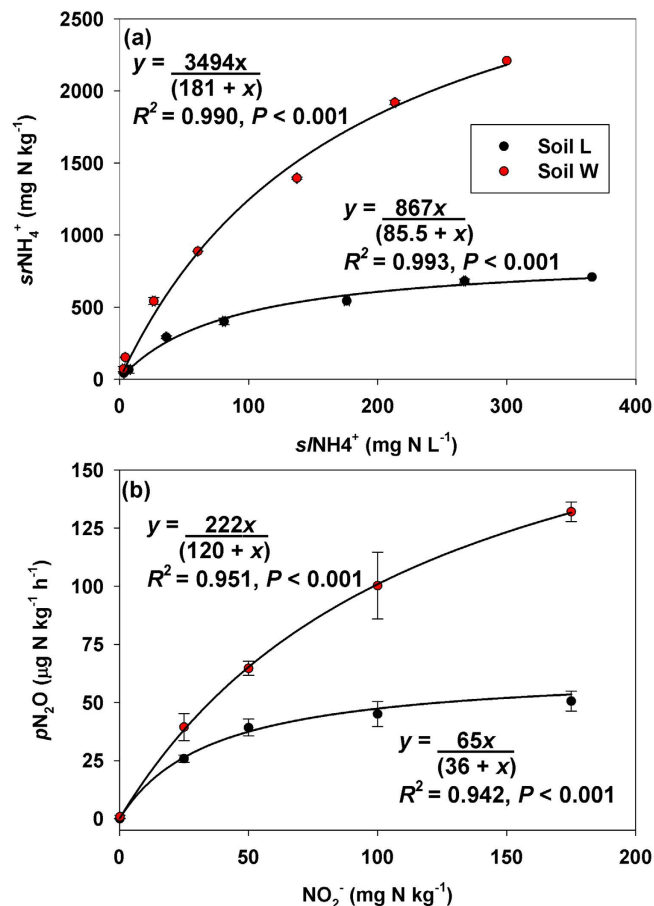


Figure 1. Ammonium sorption capacity (ACS) and potential N₂O production (pN_2O). (a) ACS results showing equilibrium NH_4^+ concentrations in sorbed-phase ($srNH_4^+$) versus solution-phase ($slNH_4^+$) and (b) pN_2O following addition of nitrite (NO_2^-) at 85% field capacity for soils L and W. Symbols are means with vertical standard error bars and lines are regression curves based on replicated data (in form of Eq. (1)). Horizontal error bars are displayed in (a) but are barely visible.

the presence of sufficiently high NH_3 levels because NOB are unable to fully process the NO_2^- produced by AOB.

However, beyond this rather general understanding of soil NO_2^- dynamics, little is known about specific soil properties that regulate NO_2^- accumulation. While related processes have been well-studied in wastewater systems¹⁴, the presence of soil surface-solution interactions and other factors complicate our understanding in soils. For example, the partitioning of NH_4^+ between soil surfaces and solution could regulate solution-phase levels and therefore influence nitrifier activity and NH_3 toxicity¹⁵. Simultaneous quantification of genes associated with activities of NOB, AOB and NH_4^+ oxidizing archaea in soil following amendment with N has been reported in a few studies^{16–18}, but more data are needed to understand the role of nitrifier responses in regulating NO_2^- and N_2O dynamics. Limited understanding of these and other factors limits our ability to predict NO_2^- dynamics for a particular soil, management practice, or climate condition, and our ability to predict N_2O emissions resulting from NO_2^- transformations^{19,20}.

In preliminary experiments, we observed that two soils collected from grazed fields in New Zealand, while having similar texture, pH, C content and C/N ratio, displayed substantially different N_2O production rates when amended with Ur. Our general hypothesis was that differences in NO_2^- dynamics were responsible for the contrasting N_2O production. In this study, we conducted a series of experiments designed to elucidate controls over NO_2^- and N_2O production under conditions representative of concentrated BU patches or Ur bands, and to explain the differences in N_2O production between these soils.

Results

Ammonium sorption. Ammonium sorption, determined in batch equilibrium experiments and modeled using Eq. 1, was significantly greater in soil W, which sorbed more NH_4^+ from solution compared to soil L (Fig. 1a). The modeled sorption parameters μ and K in soil W were four and two times greater, respectively, than in soil L (Fig. 1a).

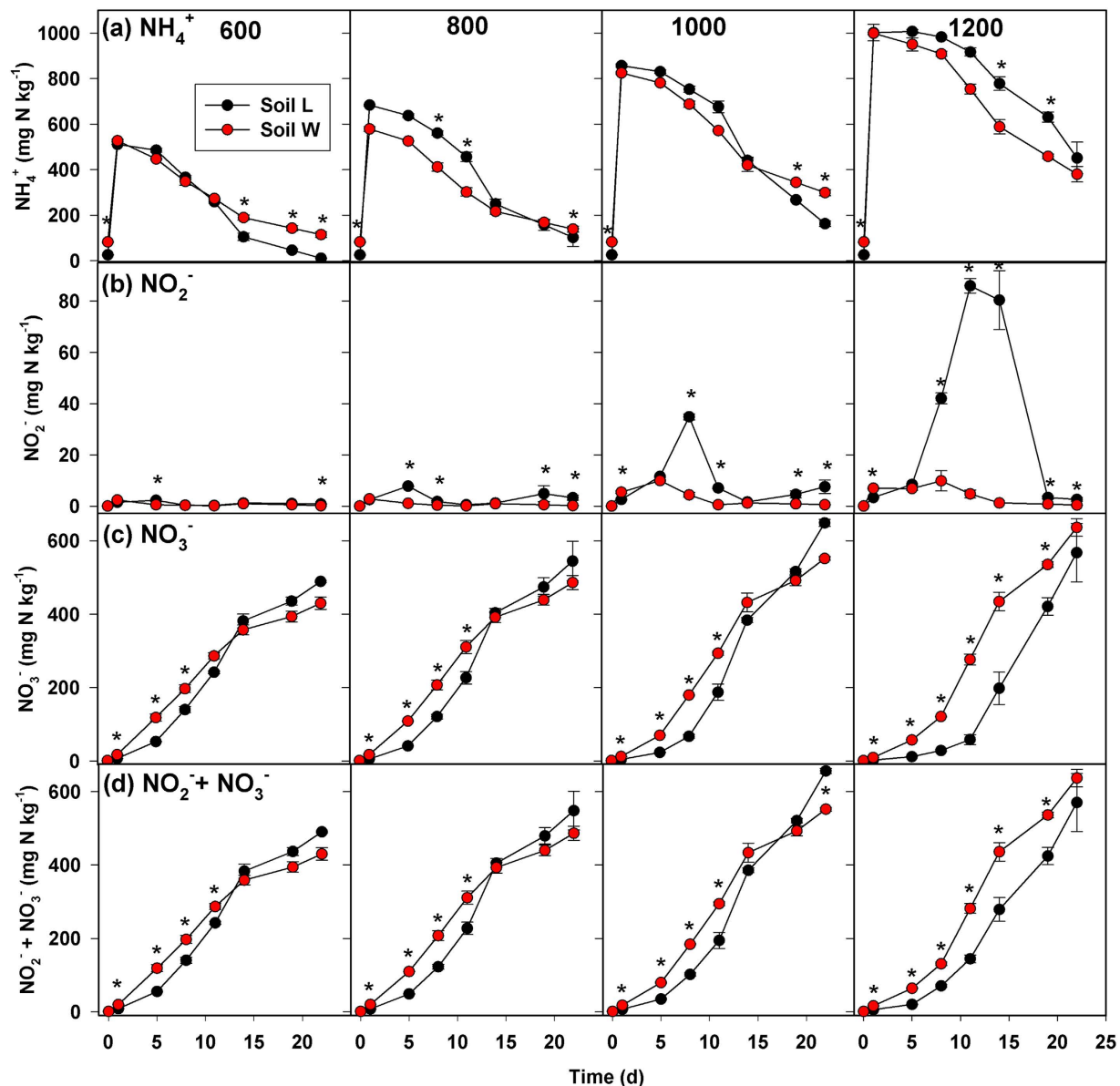


Figure 2. Results of Series 1 microcosm experiment. Concentrations of extractable (a) NH_4^+ , (b) NO_2^- , (c) NO_3^- and (d) $\text{NO}_2^- + \text{NO}_3^-$ following addition of bovine urine at 600, 800, 1000 and 1200 mg N kg^{-1} at 85% field capacity. Asterisks indicate significant differences between soils at $P < 0.05$ for a given sampling date.

Nitrite addition experiments. Soil W produced more N_2O after amendment with NO_2^- compared to soil L. The potential N_2O production rate ($p\text{N}_2\text{O}$) was well-described by models in the form of Eq. (1) with sorbed-phase NH_4^+ ($s\text{rNH}_4^+$) replaced by potential N_2O production rate ($p\text{N}_2\text{O}$), and with solution phase NH_4^+ ($s\text{NH}_4^+$) replaced by NO_2^- concentration (Fig. 1b). The modeled μ and K parameters in soil W were each approximately three times greater than in soil L.

Microcosm experiments. *Series 1 - Effect of BU addition rate at 85% of field capacity (FC).* There were significant soil-by-BU addition rate-by-time interaction effects on all point-in-time (Figs 2, 3) and cumulative variables (Table 1). Most notably for point-in-time concentrations, soil L had greater NO_2^- and actual N_2O production rate ($a\text{N}_2\text{O}$) compared to W on at least two sampling dates at all N rates, and the frequency and magnitude of significant differences in NO_2^- and $a\text{N}_2\text{O}$ by soil increased with increasing BU addition (Figs 2b, 3a). Following BU addition, both soils showed a similar temporal pattern of increasing total extractable NH_4^+ ($t\text{NH}_4^+$) followed by decreasing $t\text{NH}_4^+$ (Fig. 2a). Differences in $t\text{NH}_4^+$ by soil were not observed until at least Day 8, and the timing and direction of significant differences varied by BU addition rate. Soil W had more nitrate (NO_3^-) and ($\text{NO}_2^- + \text{NO}_3^-$) present compared to soil L during at least the first 8 d, and the magnitude and duration of significant differences

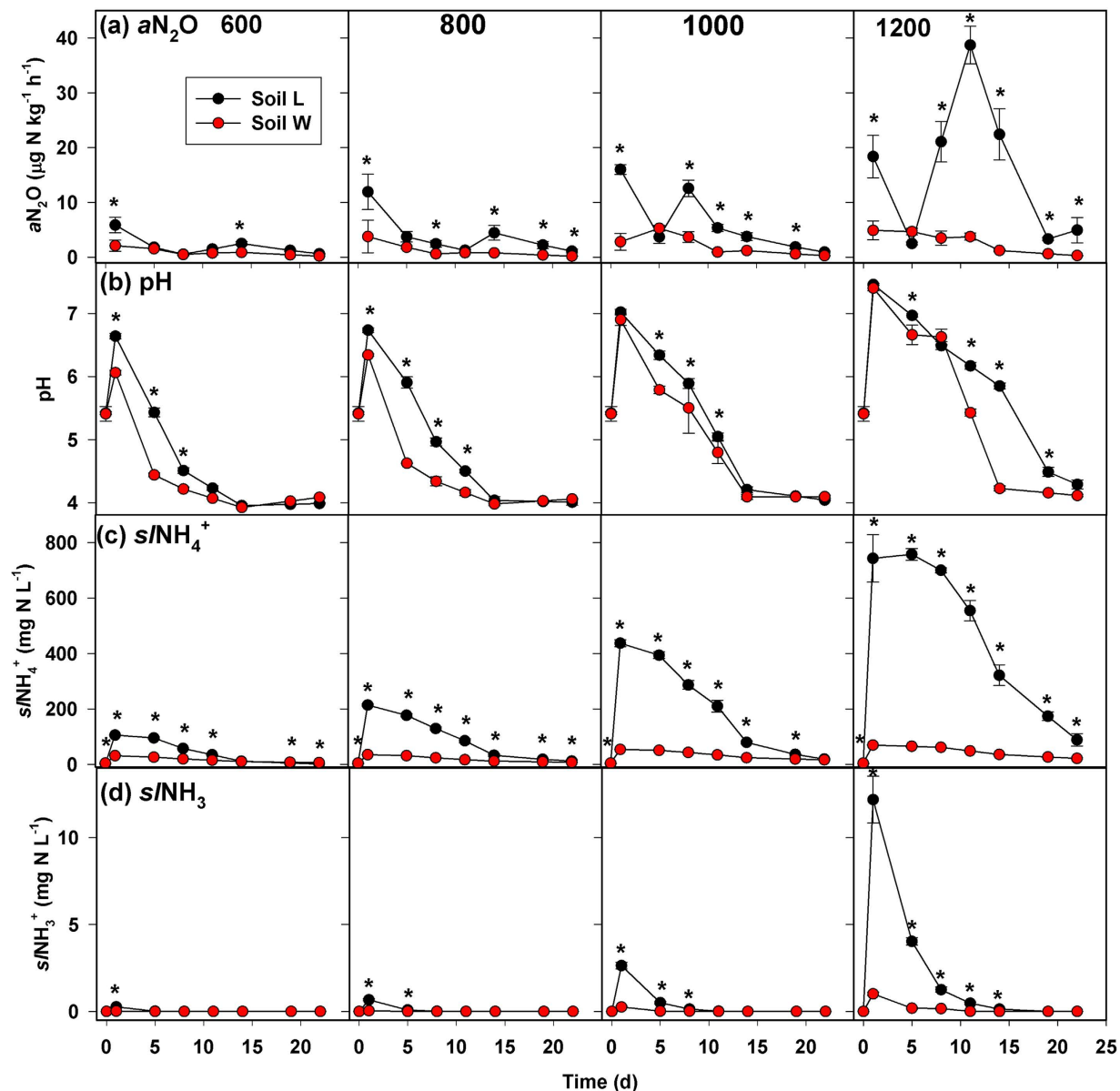


Figure 3. Results of Series 1 microcosm experiment (continued). (a) Actual N_2O production rate ($a\text{N}_2\text{O}$), (b) pH, and theoretical concentrations of solution-phase (c) ammonium (s/NH_4^+) and (d) ammonia (s/NH_3) following addition of bovine urine at 600, 800, 1000 and 1200 mg N kg^{-1} at 85% field capacity. Asterisks indicate significant differences between soils at $P < 0.05$ for a given sampling date.

in NO_3^- by soil increased with increasing BU addition (Figs 2c–d). Soil *L* consistently produced more N_2O on Day 1 compared to *W*. Soil pH, s/NH_4^+ and s/NH_3 were frequently greater in soil *L* compared to *W* (Figs 3b–d). Most notably for cumulative indices (Table 1), soil *L* had consistently greater $c\text{-NO}_2^-$, $c\text{-s}/\text{NH}_4^+$, $c\text{-NH}_3$, and $c\text{-}a\text{N}_2\text{O}$ compared to *W* at all BU addition rates. During the first 5 d, soil *W* had greater $\text{NO}_2^- + \text{NO}_3^-$ accumulation rate (NAR) compared to soil *L* at all BU addition rates, and both soils showed reduced NAR at $\text{N} \geq 1000 \text{ mg N kg}^{-1}$ compared to $\text{N} < 1000 \text{ mg N kg}^{-1}$ (Table S1). During Days 5 through 11, significant differences in NAR by soil were only present at 1000 and 1200 mg N kg^{-1} . During Days 11 through 19, soil *L* had greater NAR compared to *W* at all BU addition rates except 1200 mg N kg^{-1} .

Series 2 - Effect of soil water content with 1000 mg N kg^{-1} of BU added. There were significant soil-by-water content-by-time interaction effects on point-in-time concentrations of $t\text{NH}_4^+$, NO_2^- , NO_3^- , $a\text{N}_2\text{O}$, s/NH_4^+ , and s/NH_3 . Differences by soil in the 100% of FC treatment were similar to differences by soil in the 85% of FC treatment with 1000 mg N kg^{-1} , except for pH and $\text{NO}_2^- + \text{NO}_3^-$ where no differences were observed (Fig. 4). For cumulative indices, there were significant soil-by-water content-by-time interaction effects on $c\text{-}t\text{NH}_4^+$, $c\text{-(NO}_2^- + \text{NO}_3^-)$, $c\text{-}s/\text{NH}_4^+$ and $c\text{-}a\text{N}_2\text{O}$ (Table S2).

Soil	BU added (mg N kg ⁻¹)			
	600	800	1000	1200
<i>c-t</i> NH ₄ ⁺ (g N d kg ⁻¹)				
<i>L</i>	5.48 D‡	8.78 C	12.42 B	18.05 A
<i>W</i>	6.28 D	7.21 C	12.12 B	15.61 A
<i>P</i> > <i>t</i>	<0.001§	<0.001	0.216	<0.001
<i>c-NO</i> ₂ ⁻ (mg N d kg ⁻¹)				
<i>L</i>	23.95 D	59.55 C	209.37 B	761.04 A
<i>W</i>	15.43 B	18.72 B	72.64 A	94.38 A
<i>P</i> > <i>t</i>	0.005	<0.001	<0.001	<0.001
<i>c-NO</i> ₃ ⁻ (g N d kg ⁻¹)				
<i>L</i>	5.35 A	5.53 A	5.43 A	3.64 B
<i>W</i>	5.56 B	6.03 AB	6.22 AB	6.25 A
<i>P</i> > <i>t</i>	0.502	0.128	0.023	<0.001
<i>c-(NO</i> ₂ ⁻ + <i>NO</i> ₃ ⁻) (g N d kg ⁻¹)				
<i>L</i>	5.38 A	5.59 A	5.64 A	4.40 B
<i>W</i>	5.57 B	6.05AB	6.29 A	6.35 A
<i>P</i> > <i>t</i>	0.448	0.102	0.029	<0.001
<i>c-H</i> ⁺ (mol H ⁺ d kg ⁻¹)				
<i>L</i>	0.315 A	0.295 A	0.256 B	0.129 C
<i>W</i>	0.267 A	0.274 A	0.243AB	0.221 B
<i>P</i> > <i>t</i>	0.010	0.217	0.433	<0.001
<i>c-aN</i> ₂ O (mg N ₂ O-N kg ⁻¹)				
<i>L</i>	0.90 D	1.72 C	2.90 B	8.08 A
<i>W</i>	0.44 B	0.52 B	1.10 A	1.29 A
<i>P</i> > <i>t</i>	0.005	<0.001	<0.001	<0.001
<i>c-s</i> NH ₄ ⁺ (g N d kg ⁻¹)				
<i>L</i>	0.94 D	2.02 C	4.45 B	10.29 A
<i>W</i>	0.35 C	0.41 C	0.74 B	1.01 A
<i>P</i> > <i>t</i>	0.020	<0.001	<0.001	<0.001
<i>c-s</i> NH ₃ (mg N d kg ⁻¹)				
<i>L</i>	0.72 D	1.99 C	8.79 B	50.26 A
<i>W</i>	0.055 C	0.11 C	0.76 B	3.70 A
<i>P</i> > <i>t</i>	<0.001	<0.001	<0.001	<0.001

Table 1. Cumulative indices for total extractable ammonium (*c-t*NH₄⁺), nitrite (*c-NO*₂⁻), nitrate (*c-NO*₃⁻), the sum of nitrite and nitrate (*c- [NO*₂⁻ + *NO*₃⁻]), actual N₂O production rate (*c-aN*₂O), acidity (*c-H*⁺) and solution-phase ammonium (*c-s*/NH₄⁺) and ammonia (*c-s*/NH₃) as affected by soil type and rate of bovine urine (BU) in Series 1 experiments. Statistical analyses are based on logarithm base 10 transformed data, and back-transformed means are reported. ‡Within a row, means followed by the same letter are not significantly different at *P* ≤ 0.05. §Significance of *t* test comparing the means from the two soils for a given rate of BU addition.

Differences in *c-aN*₂O by soil were similar at 85% and 100% of FC, but both soils had greater *c-aN*₂O at 100% compared to 85% of FC. Across both soils, *c-NO*₂⁻ and *c-s*/NH₃ were greater at 100% compared to 85% of FC, while *c-NO*₃⁻ and *c-H*⁺ were greater at 85% compared to 100% of FC (Table S3). Across both water content treatments, *c-NO*₂⁻ was greater in soil *L* compared to *W*.

Series 3- Effect of BU versus Ur added at 1000 µg N g⁻¹ at 85% of FC. There were significant soil-by-N source-by-time interaction effects on all point-in-time variables, and differences by soil following Ur addition were generally consistent with differences following BU addition at 1000 mg N kg⁻¹ (Fig. 4). However, differences by soil tended to be more consistent and/or to persist longer with Ur compared to BU. Also, *t*NH₄⁺ and pH each took longer to reach their maximum values and did not decrease as rapidly with Ur compared to BU. Cumulative *t*NH₄⁺, *c-N*₂O, and *c-s*/NH₃ were greater with Ur, while *c-H*⁺ was

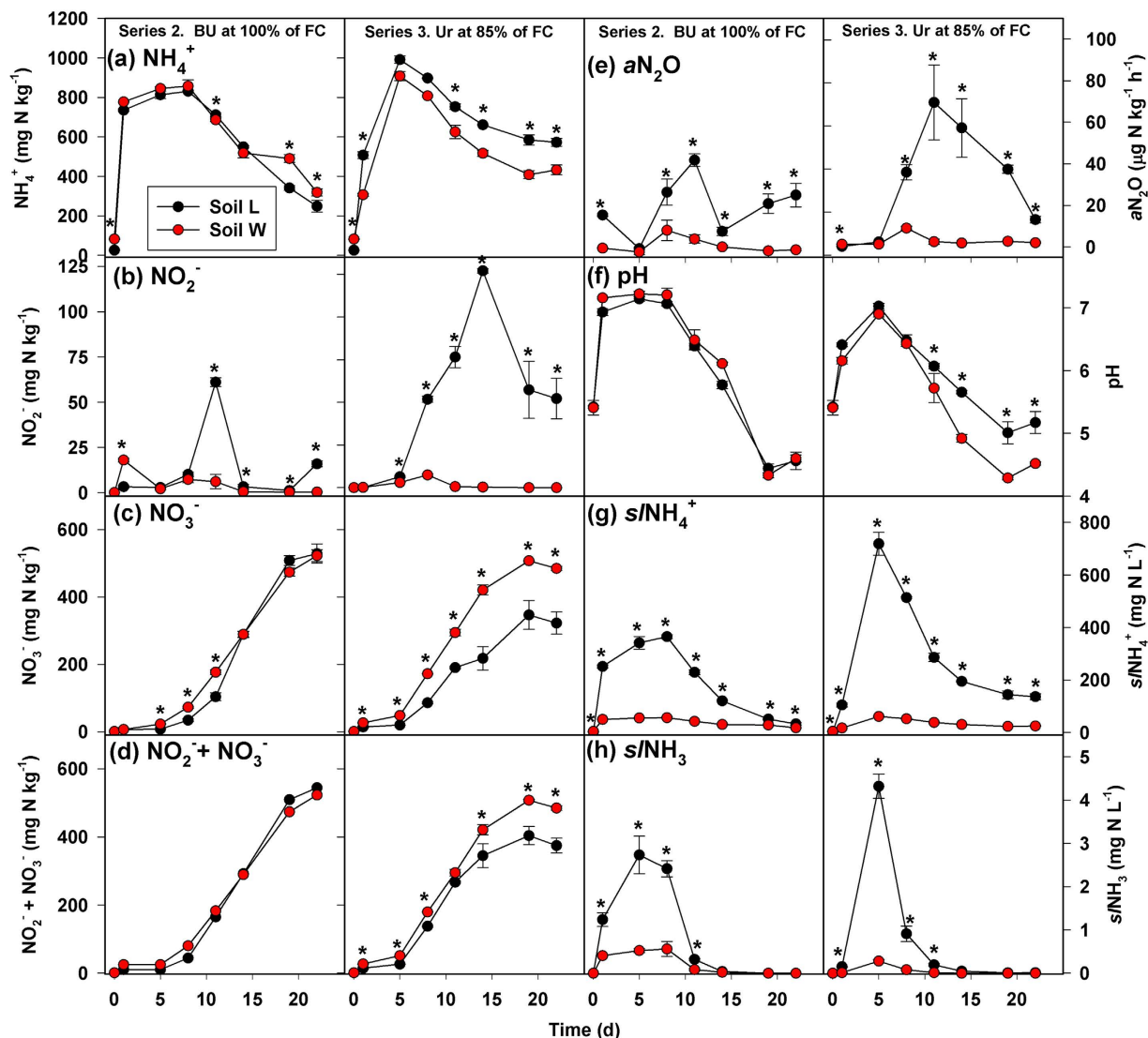


Figure 4. Results of Series 2 and 3 microcosm experiments. Concentrations of extractable (a) NH_4^+ , (b) NO_2^- , (c) NO_3^- and (d) $\text{NO}_2^- + \text{NO}_3^-$, (e) actual N_2O production rate ($a\text{N}_2\text{O}$), (f) pH and theoretical concentrations of solution-phase (g) ammonium ($s\text{NH}_4^+$) and (h) ammonia ($s\text{NH}_3$) in Series 2 (left-hand plates for each variable) and Series 3 (right-hand plates). Series 2 used bovine urine (BU) at 1000 mg N kg^{-1} with soils at 100% of field capacity (FC), and Series 3 used urea (Ur) at 1000 mg N kg^{-1} with soils at 85% of FC. Asterisks indicate significant differences between soils at $P < 0.05$ for a given sampling date.

lower with Ur, compared with BU, in both soils (Table S4). Cumulative NO_2^- was more than five times greater with Ur compared to BU for soil L.

Gene copies of bacterial ammonia monooxygenase (*amoA-b*) associated with AOB were greater in soil L compared to W, but increased over time in a similar manner in both soils until Day 14, after which the abundances did not change (Fig. 5). There was a significant soil-by-time interaction effect on gene copies of archaeal ammonia monooxygenase (*amoA-a*), but a difference by soil was observed only on the final sampling date (Fig. 5b). In both soils, *amoA-a* numbers did not change until after Day 14, corresponding to the cessation of any increases in *amoA-b*. Most notable was a significant soil-by-time interaction effect on gene copies of bacterial nitrite oxidoreductase (*nxrA*) associated with NOB ($P < 0.001$), which were initially lower in soil W than L, and subsequently increased in soil W by a factor of 60 while remaining static in soil L (Fig. 5c).

Correlation and regression analyses. Soil NO_2^- was positively correlated with $t\text{NH}_4^+$, $s\text{NH}_4^+$ and $s\text{NH}_3$, and $c\text{-NO}_2^-$ was positively correlated with $c\text{-}t\text{NH}_4^+$, $c\text{-}s\text{NH}_4^+$ and $c\text{-}s\text{NH}_3$ (Table S5). Across all experiments (Series 1-3), $c\text{-NO}_2^-$ was most strongly correlated with $c\text{-}s\text{NH}_3$, which explained 87% of the total variance in $c\text{-NO}_2^-$ (Fig. 6a). Soil NO_2^- was also positively correlated with $a\text{N}_2\text{O}$, and $c\text{-NO}_2^-$ was

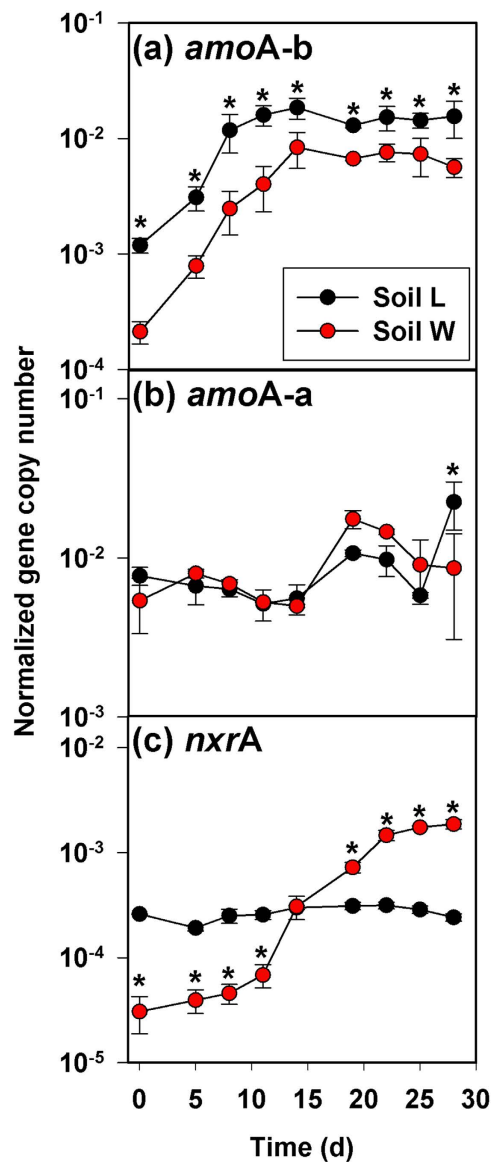


Figure 5. Gene copy abundances in Series 3 microcosm experiment. (a) *amoA-b*, (a) *amoA-a*, and (c) *nxrA* following addition of Ur at $1000 \text{ mg N kg}^{-1}$ soil with soils at 85% of FC. Asterisks indicate significant differences between soils at $P < 0.05$. Normalized gene abundances are expressed relative to the number of copies of prokaryotic (bacteria + archaea) 16S rRNA genes in each sample⁴⁷.

positively correlated with *c-aN₂O*. Across all experiments, *c-NO₂⁻* explained 82% of the total variance in *c-aN₂O* (Fig. 6b). Soil *NO₃⁻* and (*NO₂⁻* + *NO₃⁻*) tended to be negatively correlated with *N₂O* (Table S5). Multiple regression models with *c-sNH₄⁺* and *c-H⁺* as independent variables explained 93 and 89% of the variance in *c-NO₂⁻* and *c-aN₂O*, respectively (Figs 5c,d).

Discussion

This is the first study to correlate the dynamics of *sNH₃*, *NO₂⁻*, *N₂O* and nitrifier genes in incubating soil. The strong relationship ($r^2 = 0.87$) between *c-sNH₃* and *c-NO₂⁻* suggests that *NH₃* toxicity acting more strongly on NOB than AOB, and more strongly in soil *L* than in soil *W*, was responsible for the contrasting *NO₂⁻* and *N₂O* dynamics in the two soils^{11–14}. The greater *N₂O* production in soil *L* appeared to be driven by a greater *NO₂⁻* accumulation which in turn resulted from greater *sNH₃* accumulation due to its lower ASC (Fig. 7). This explanation is further supported by the static *nxrA* gene copies in soil *L* in contrast to substantial increases in *nxrA* observed in soil *W*.

Differences in ASC were related to differences in cation exchange capacity (CEC); i.e., the ratio (*W:L*) of K_d values in the two soils was 1.91 which was nearly identical to the ratio of their CEC values (1.93). Thus, while soil *L* and *W* had similar organic C and clay contents, differences in ASC were likely due to differences in chemical composition of soil organic matter and/or mineralogical composition of clay

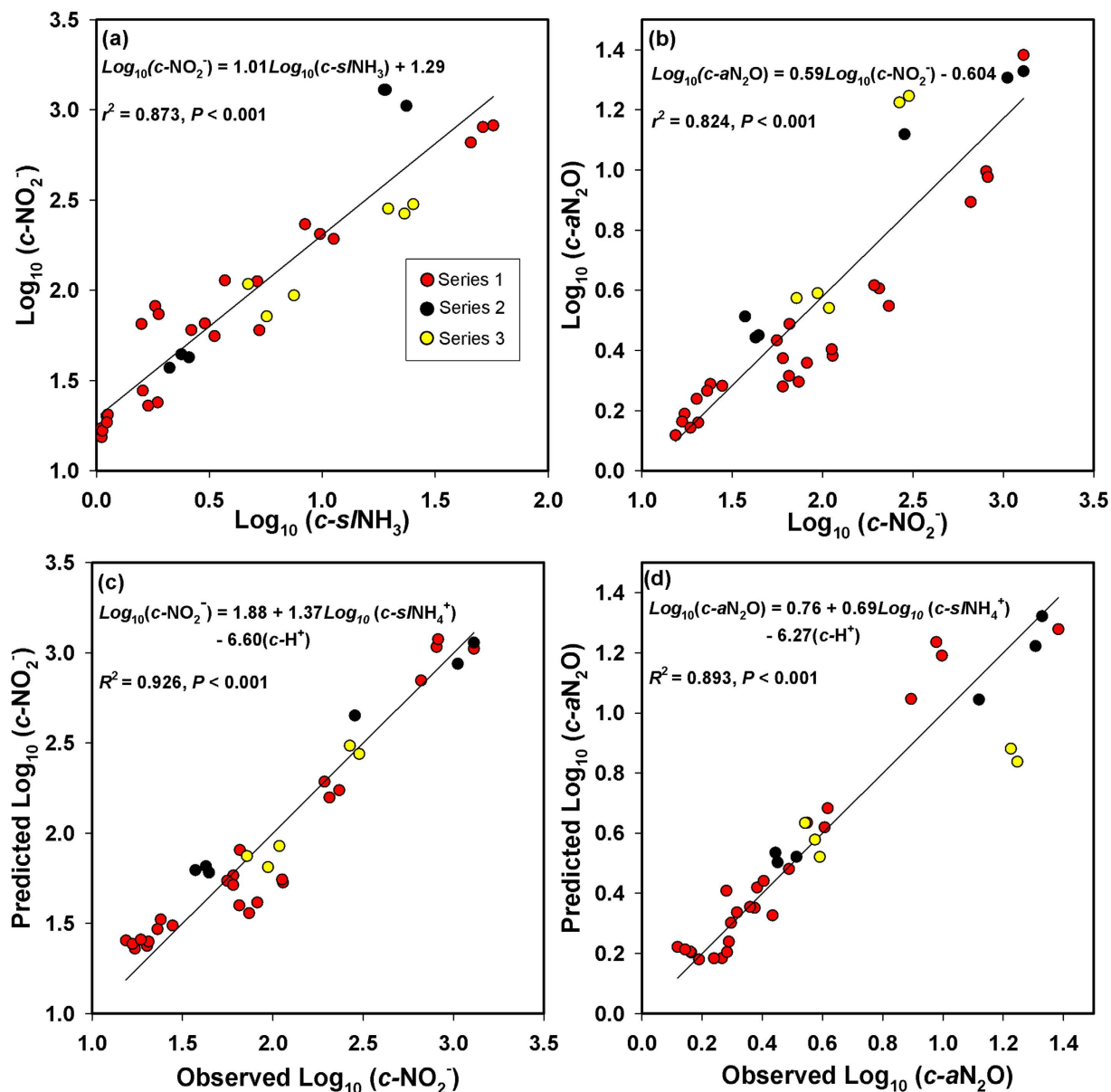


Figure 6. Regression results. Single-factor regression models of (a) cumulative nitrite ($c\text{-NO}_2^-$) versus cumulative solution-phase ammonia ($c\text{-s/NH}_3$) and (b) cumulative actual N_2O production ($c\text{-aN}_2\text{O}$) versus $c\text{-NO}_2^-$ with regression lines, and multiple regression models describing (c) $c\text{-NO}_2^-$ and (d) $c\text{-aN}_2\text{O}$ as functions of cumulative solution-phase ammonium ($c\text{-s/NH}_4^+$) and cumulative acidity ($c\text{-H}^+$) with 1:1 lines, for all microcosm data (Series 1–3).

which control CEC²¹. It is not likely that a difference in the capacity of the two soils to fix N in clay minerals was an important factor; because NH_4^+ fixed by clay is not readily extracted by 2 M KCl nor is it readily available to microbes, such an effect would have been evident in differences by soil in $t\text{NH}_4^+$ that were not associated with differences in NAR and/or urea hydrolysis rates²².

Our calculations of $s\text{NH}_3$ concentrations are theoretical approximations. Because soil pH is by its nature operationally defined, any subsequent calculations are also operationally defined; e.g., a different range of absolute NH_3 values would have resulted if a different pH solvent were used²³, although $s\text{NH}_3$ levels based on a single solvent provide a basis for relative comparison. Our methods assumed that the NH_4^+ -sorption equilibria in the isotherm experiments also described the solid-liquid NH_4^+ partitioning in the microcosm experiments. Nonetheless, it is interesting that the maximum $s\text{NH}_3$ concentrations observed in soil L (approximately 0.5 to 10 mg N L⁻¹) were within the range observed to inhibit NOB and cause NO_2^- accumulation in nitrifying wastewater systems¹⁴. Apart from any theoretical $s\text{NH}_3$ calculations, the multiple regression model (Fig. 6c) is further suggestive of NH_3 toxicity; that is, increased

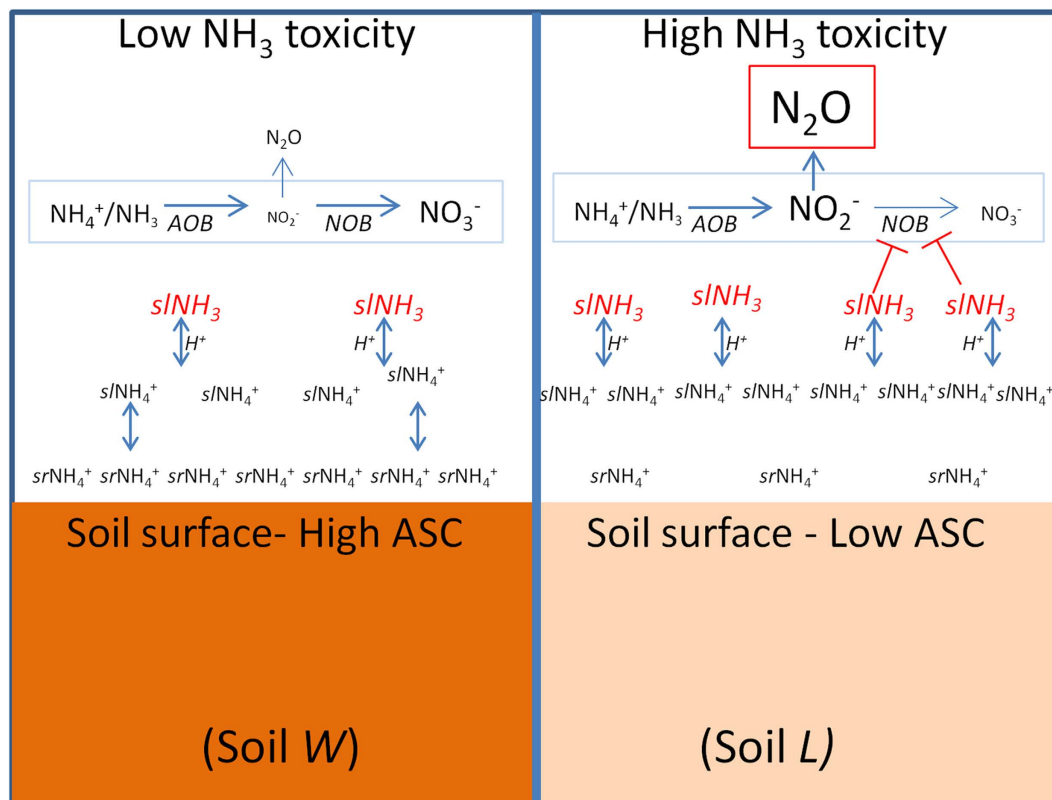


Figure 7. Conceptual schematic. Decreased ammonium (NH₄⁺) sorption capacity (ASC) results in increased ratio between solution-phase (*sl*) and sorbed-phase (*sr*) NH₄⁺, which increases the potential formation of free ammonia (*sl*NH₃). When *sl*NH₃ differentially inhibits nitrite (NO₂⁻) oxidizing bacteria (NOB) to a greater extent than NH₃ ammonia-oxidizing bacteria (AOB), NO₂⁻ accumulates, leading to increased NO₂⁻-driven N₂O production in the low ASC soil.

*sl*NH₄⁺ combined with reduced acidity (which together are the ‘raw ingredients’ for NH₃ formation) explained 93% of the variance in *c*-NO₂⁻.

The *sl*NH₃ levels reached maximum values the day after N addition, but NO₂⁻ did not reach maxima until at least Day 5 and generally remained elevated for longer than *sl*NH₃. These results are reflected in stronger correlations between *c*-NH₃ and *c*-NO₂⁻ compared with correlations between point-in-time concentrations. This result could have been due to residual inhibitory effects of *sl*NH₃ on NOB that persisted even after *sl*NH₃ had subsided. It also is possible that once NO₂⁻ started to accumulate, NO₂⁻ itself (or its protonated form [HNO₂]) became a source of toxicity to NOB. Kinetic models that account for NH₃ and NO₂⁻/HNO₂ as separate sources of toxicity affecting AOB and NOB have been developed for wastewater systems¹⁴.

Previous studies have found a significant correlation between NO₂⁻ and N₂O dynamics^{9,11,24}. The NO₂⁻ molecule is an immediate precursor substrate for N₂O produced via nitrifier-denitrification¹⁹ and chemo-denitrification^{20,25}, and there is evidence that N₂O can be produced via reaction of NO₂⁻ with hydroxylamine (NH₂OH)²⁶. Previous studies have also found significant differences among soils in *p*N₂O following amendment with NO₂⁻^{20,27}. The current results show that *p*N₂O is not necessarily a reliable indicator of actual N₂O production (*a*N₂O) following amendment of soil with BU or Ur; i.e., although soil *W* had greater *p*N₂O after being artificially amended with NO₂⁻, soil *L* had greater *a*N₂O because it accumulated more NO₂⁻ biologically than soil *W* following amendment with BU or Ur.

These experiments were not designed to precisely distinguish among all potential pathways of N₂O production, e.g. nitrification, nitrifier-denitrification, heterotrophic denitrification, or chemodenitrification^{19,20,28,29}. The experiments were designed to maintain aerobic conditions, and therefore the influence of denitrification of NO₃⁻ as an N₂O source was expected to be minimal. This was supported by the lack of positive correlation between *a*N₂O and soil NO₃⁻ levels; in fact, NO₃⁻ was negatively correlated with *a*N₂O in many cases. A previous study²⁰ found that headspace O₂ levels <5% were required for N₂O production to proceed in NO₃⁻-amended soil; in contrast, NO₂⁻-amended soil readily produced N₂O at ambient O₂ and displayed increasing N₂O per unit NO₂⁻ as O₂ decreased below 20%. Similar findings have been shown in culture studies examining nitrifier-denitrification³⁰. Thus, in the current study, greater N₂O production at greater water content was likely due to N₂O derived from

nitrifier-denitrification. At 100% of FC, nitrification proceeded more slowly than at 85% of FC, possibly due decreased O₂ availability to support NH₄⁺ oxidation. Because *t*NH₄⁺ and pH did not decrease as quickly (owing to slower nitrification-induced H⁺ production), this resulted in greater *s*/NH₃, which in turn could have caused the greater NO₂⁻ at 100% of FC compared to 85% of FC. Thus, greater availability of NO₂⁻, as well as increased potential for nitrifier-denitrification to produce N₂O with reduced O₂, likely enhanced N₂O at 100% of FC.

Both soils responded differently to Ur compared to BU. With BU, it took 1 d for *t*NH₄⁺ and pH to reach their maximum values compared to 5 d with Ur; this was likely due to compounds such as hippuric acid present in BU which accelerate Ur hydrolysis³¹. Soil pH also remained elevated for a longer period with Ur (again, indicating slower nitrification-induced H⁺ production), which resulted in a doubling of *c*-*s*/NH₃ compared to BU. In soil *L*, this resulted in a 4- to 5-fold increase in NO₂⁻ and a 7-fold increase in *c*-N₂O. These results highlight the interactions involving several processes and substrates following BU and Ur addition that can regulate N₂O production.

On the first day following addition of BU to soil *L* (in Series 1 and 2), N₂O production was elevated without a corresponding increase in soil NO₂⁻ or NO₃⁻, and then declined on Day 3. This result was not observed with Ur, nor was it observed with soil *W*. Further research would be needed to explain this result, but it is possible that any NO₂⁻ produced during the initial onset of nitrification was consumed in the N₂O-producing reactions and therefore was not measurable. Urine addition could have stimulated 'co-denitrification' reactions³², or alternatively, N₂O may have been produced from reactions involving NH₂OH produced during AOB activity²⁸.

While NH₃ is the main substrate utilized by AOB³³, at higher levels, NH₃ can itself inhibit AOB activity. Decreasing NAR with increasing *s*/NH₃ was observed in a grassland soil amended with BU and attributed to NH₃ toxicity effects on AOB³⁴. Similar results were found for NAR in Series 1 during Days 0–5. The qPCR data from Series 3 indicate that any NH₃ toxicity effects on AOB were not large enough to inhibit *amoA*-b genes from increasing during Days 0–14. The *amoA* data also are consistent with results in New Zealand grasslands soils³⁵, where *amoA*-b genes increased following N addition but *amoA*-a genes did not. Here, we found an increase in *amoA*-a numbers occurred only after *amoA*-b gene copies stopped increasing. This could indicate that *amoA*-b growth was inhibited after Day 14 by increasing acidity³⁶ or NO₂⁻/HNO₂¹⁴ which might have favored *amoA*-a activity.

These results have implications for increased fundamental understanding as well as pointing in new directions for modeling and mitigating N₂O emissions. The current experiments were aimed at studying processes occurring in localized zones receiving concentrated N inputs representative of potential N₂O production hot spots. Under field conditions, these processes may be further modified by water infiltration or evaporation, temperature dynamics and other factors. Nonetheless, this study shows that soils having largely similar physical and chemical properties but differing in ASC can display dramatically different potentials for NH₃ toxicity, NO₂⁻ accumulation and N₂O production. A previous study showed effects of altering CEC on nitrification dynamics¹⁵, but effects on NO₂⁻ or N₂O dynamics have not been considered. Further research comparing soils differing in ASC, and examining the effects of altering soil CEC, should be performed under both lab and field conditions to further investigate these variables as modeling parameters and potential N₂O mitigation factors.

Methods

Soils. Soil '*L*' was collected from a research field at Lincoln University, New Zealand (43.648 S; 172.454 E) that had been under pasture (*Lolium perenne* L.) for at least 5 yr. Soil '*W*' was collected from a farmer's field east of Waikari, New Zealand (42.964 S; 172.629 E) planted to alfalfa (*Medicago sativa* L.) and rotationally grazed by sheep (*Ovis aries*). Soils were collected from the upper 0.10 m and allowed to dry at 25 °C, and then ground and sieved (2 mm). Soils *L* and *W* were both classified as silt loams and had similar clay content (116 and 130 g kg⁻¹, respectively), organic C (26, 33 g kg⁻¹), C/N ratio (11.2, 10.6), and pH in H₂O (6.3, 6.1), but differing CEC (14 and 27 cmol_c kg⁻¹) (Table S6).

Ammonium sorption capacity and solution-phase concentrations. Ammonium sorption isotherms were obtained using a batch equilibrium method³⁷. Solutions (15 mL) containing NH₄⁺ as NH₄Cl (5, 10, 50, 100, 200, 300 and 400 mg NH₄⁺-N L⁻¹) were added to 50-mL polyethylene tubes containing 0.75 g soil. Three replicate tubes of each NH₄⁺ concentration were equilibrated on a reciprocating shaker for 18 h at 100 rpm. Mixtures were filtered (Whatman 42) and the filtrate analyzed for NH₄⁺³⁸ with a flow-injection analyzer (FIA) (Lachat QuikChem 8500 or Alpkem FS3000). The amount of *sr*NH₄⁺ was calculated from the difference in *s*/NH₄⁺ at the beginning and end of equilibration and accounting for the initial 2 M KCl-extractable NH₄⁺ content of the soil. The resulting data were not consistent (*R*² < 0.6) with commonly used models³⁹ but were well-described (*R*² ≥ 0.99) by models of the form

$$srNH_4^+ = \frac{\mu (s/NH_4^+)}{K + (s/NH_4^+)} \quad (1)$$

where μ (mg N kg^{-1}) is the maximum sorption capacity and K (mg N L^{-1}) is the $s\text{NH}_4^+$ concentration at which $sr\text{NH}_4^+$ equals one-half of μ . Eq. (1) is similar in form to the Langmuir model and has a 'linear portion' for the case where $s\text{NH}_4^+ \ll K$, such that $sr\text{NH}_4^+ = (s\text{NH}_4^+)$ where $K_d = \mu/K$ is the slope with units (L kg^{-1}). Eq. (1) was used to calculate theoretical concentrations of $s\text{NH}_4^+$ and $s\text{NH}_3$ by expressing the total extractable ammonium ($t\text{NH}_4^+$, mg N kg^{-1}) under equilibrium conditions as follows:

$$t\text{NH}_4^+ = sr\text{NH}_4^+ + \theta (s\text{NH}_4^+) + \theta (s\text{NH}_3) \quad (2)$$

where θ is the soil water content (L kg^{-1}). Eq. (1) was used to replace $sr\text{NH}_4^+$ in Eq. (2), and $s\text{NH}_3$ in Eq. (2) was replaced by:

$$s\text{NH}_3 = (s\text{NH}_4^+) K_A 10^{\text{pH}} \quad (3)$$

where K_A is the acid dissociation constant (9.245) for the $\text{NH}_4^+ - \text{NH}_3$ acid-base pair at 25°C^{40} . This resulted in the quadratic equation:

$$\sigma (s\text{NH}_4^+)^2 + \nu (s\text{NH}_4^+) + \delta = 0 \quad (4)$$

where σ , ν and δ are constants containing the parameters μ , K , θ , K_A , $t\text{NH}_4^+$ and 10^{pH} . For each sampling event, measured values of $t\text{NH}_4^+$ and pH were substituted into the constant terms, Eq. (4) was solved for $s\text{NH}_4^+$ using the quadratic formula, and $s\text{NH}_3$ was calculated using Eq. (3). Example calculations are provided as Supplementary Information (SI). The above procedure was compared to another method where $\theta(s\text{NH}_3)$ was omitted from Eq. (2), and the results agreed within $<1\%$. Thus, assumptions regarding whether $s\text{NH}_3$ was captured in the $t\text{NH}_4^+$ analysis affected the results to a negligible extent.

Nitrite-addition experiments. The potential for each soil to produce N_2O when amended with NO_2^- was determined²⁰. Soil was amended with solutions containing KNO_2 to achieve concentrations of 0, 25, 50, 100 and $175 \text{ mg NO}_2^- \text{ N kg}^{-1}$ at a water content equivalent to 85% of FC. Solutions were added to 10.0 g of air-dried soil in 'wide-mouth' 250 mL glass jars (69 mm diameter by 65 mm) and homogenized with a spatula. Jars were sealed with septum-equipped caps and incubated for 1 h at 25°C with sampling of the headspace at 0, 30 and 60 min. Gas samples were immediately transferred to evacuated glass vials which were analyzed for N_2O with a gas chromatograph (8610, SRI Instruments, CA) equipped with an electron capture detector and interfaced to an autosampler (Gilson 222XL, Middleton, WI)⁴¹. The rate of increase in headspace N_2O concentration, headspace volume and soil mass were used to calculate $p\text{N}_2\text{O}^{20}$.

Microcosm experiments. Three series of microcosm experiments were conducted. Series 1 used each soil amended with four rates of BU equivalent to 600, 800, 1000 and $1200 \text{ mg N kg}^{-1}$ at a water content equivalent to 85% of FC. Series 2 used each soil amended with BU at $1000 \text{ mg N kg}^{-1}$ at 100% of FC. Series 3 used each soil amended with Ur at $1000 \text{ mg N kg}^{-1}$ at 85% of FC. At the start of the experiment, 21 replicate 250-mL glass jars of each treatment were established by adding solutions by pipette to 10.0 g of dry soil and homogenizing with a spatula such that the wetted soil occupied a thin layer ($\sim 3 \text{ mm}$) in the bottom of the jar. Three replicate jars of each treatment were sacrificed for destructive analysis after 1, 5, 8, 11, 14, 19 and 22 d. An additional three jars containing soil amended with deionized H_2O were used to represent 'Day 0'. Jars were incubated in the dark at 25°C . On each sampling day, three randomly selected jars of each treatment were opened for 5 min to equilibrate the jar headspace with lab air and then sealed with caps, equipped with rubber septa, for 1 h. The jar headspace was sampled at 0, 30 and 60 min by syringe and $a\text{N}_2\text{O}$ was determined using methods described above. Nitrous oxide measured in the microcosm experiments is referred to as 'actual' N_2O production rate ($a\text{N}_2\text{O}$) to distinguish from $p\text{N}_2\text{O}$. Immediately following gas sampling, approximately one-half of the soil mass in each jar was gravimetrically transferred to a polyethylene tube and extracted in 40 mL of 2 M KCl for 1 h. The extracts were filtered and stored at 4°C until determination of $t\text{NH}_4^{+38}$. Subsamples of the extract also were used to determine soil pH. Soil remaining in each jar was amended with 40 mL of a separate 2 M KCl solution and extracted for 10 min and then filtered for determination of NO_2^- and the sum of $\text{NO}_2^- + \text{NO}_3^-$. The pH of the 2 M KCl used for NO_2^- and $\text{NO}_2^- + \text{NO}_3^-$ extraction was adjusted so that, during extraction, the pH of the soil-solution mixture was $\geq 8.5^{42}$. The NO_2^- analysis was performed within 3 h with a spectrophotometer (Shimadzu UV mini-1240)³⁸. The $\text{NO}_2^- + \text{NO}_3^-$ analysis was conducted within 24 h using a FIA preceded by Cd-reduction of NO_3^- to NO_2^- , and NO_3^- was determined by difference³⁸.

The microcosms were designed to maintain aerobic conditions with minimal need for aeration due to the high ratio of headspace volume to soil mass and the high ratio of jar diameter to volume. The jars were opened for 10 min on Days 1, 8 and 15. This procedure minimized evaporative moisture losses while maintaining headspace O_2 above 18% as determined by gas chromatographic analysis with a thermal conductivity detector. Opening of the jars on Day 1 also allowed release of CO_2 produced during hydrolysis of Ur. Field capacities (0.35 and $0.45 \text{ kg H}_2\text{O kg}^{-1}$ for soil L and W, respectively) were determined by incremental water addition until free water was observed. Bovine urine was collected from the Lincoln University dairy farm where cows were grazing perennial ryegrass (*Lolium perenne* L.)/white

clover (*Trifolium repens* L.). Urine was kept frozen until the day prior to setting up the experiment, at which time the urine was thawed and analyzed for total N content. Appropriate volumes of BU and H₂O were added to soil in each jar to achieve target N concentrations and water contents. Because these grazed soils are commonly dry at the surface for days at a time prior to receiving urine deposition, we did not add water or pre-incubate the soils prior to amendment.

Quantitative polymerase chain reaction (qPCR). For Series 3, additional soil sub-samples were collected for DNA isolation and quantification of nitrifier gene abundances. On Days 0, 5, 8, 11, 14, 19, 22, 25 and 28, sub-samples (0.25 g) were extracted using a PowerLyzer PowerSoil DNA isolation Kit (MoBio, Carlsbad, CA) in accordance with manufacturer recommendations except for the final washing step which was performed twice rather than once. Abundances of 16S ribosomal RNA (16S rRNA), *amoA-b*, *amoA-a* and *nxrA* were determined using appropriate primers^{43–46}. Abundances of *amoA-b*, *amoA-a* and *nxrA* were normalized to recovered 16S rRNA abundances⁴⁷. Additional details are provided as SI.

Data analysis. Concentrations of all N species and production of N₂O are expressed on a dry weight soil basis. Chemical concentrations and pH determined at individual times were used to calculate cumulative 'exposure' indices using trapezoidal integration of concentration versus time data^{7,9,48}. We use a 'c-' prefix to distinguish cumulative variables (e.g. *c*-NO₂⁻) from point-in-time concentrations (e.g. NO₂⁻). For cumulative acidity (*c*-H⁺), pH was first converted to theoretical hydrogen ion concentration using H⁺ = 10^{-pH} prior to integration. Integration of *a*N₂O versus time also was performed, but in this case the resulting variable (*c*-*a*N₂O) represents cumulative N₂O production. The NAR was calculated over different time intervals from the difference in NO₂⁻+NO₃⁻ concentration divided by elapsed time. Three sets of data from the microcosm experiments were analyzed independently. The first set included all data from Series 1, the second set included data from Series 2 plus the 1000 mg N kg⁻¹ treatment from Series 1 (to examine water content effects) and the third set included data from Series 3 plus the 1000 mg N kg⁻¹ treatment from Series 1 (to examine N source effects). Each set was analyzed as a completely randomized design at *P* ≤ 0.05 using the MIXED procedure of SAS [Version 9.2, SAS Institute, Cary, NC] with time as a repeated measurement. Additional details are provided as SI.

References

- Del Grosso, S. J. *et al.* Global scale DAYCENT model analysis of greenhouse gas emissions and mitigation strategies for cropped soils. *Global Planet. Change.* **67**, 44–50 (2009).
- Vogeler, I., Giltrap, D. & Cichota, R. Comparison of APSIM and DNDC simulations of nitrogen transformations and N₂O emissions. *Sci. Total Environ.* **465**, 147–155 (2013).
- Haynes, R. J. & Williams, P. H. Nutrient cycling and soil fertility in the grazed pasture ecosystem. *Adv. Agron.* **49**, 119–199 (1993).
- Flessa, H., Dorsch, P., Beese, F., König, H. & Bouwman, A. F. Influence of cattle wastes on nitrous oxide and methane fluxes in pasture land. *J. Environ. Qual.* **6**, 1366–1370 (1996).
- Wetselaar, R., Passioura, J. B. & Singh, B. R. Consequences of banding nitrogen fertilizers in soil. i. Effects on nitrification. *Plant Soil.* **36**, 159–175 (1972).
- Singh, Yadvinder & Beauchamp, E. G. Nitrogen transformations near urea in soil: effects of nitrification inhibition, nitrifier activity and liming. *Fert. Res.* **18**, 201–212 (1989).
- Engel, R., Liang, D. L., Wallander, R. & Bembek, A. Influence of urea fertilizer placement on nitrous oxide production from a silt loam soil. *J. Environ. Qual.* **39**, 115–125 (2010).
- Halvorson, A. D. & Del Grosso, S. J. Nitrogen placement and source effects on nitrous oxide emissions and yields of irrigated corn. *J. Environ. Qual.* **42**, 312–322 (2013).
- Maharjan, B. & Venterea, R. T. Nitrite intensity explains N management effects on N₂O emissions in maize. *Soil Biol. Biochem.* **66**, 229–238 (2013).
- Khan, S., Clough, T. J., Goh, K. M. & Sherlock, R. R. Nitric and nitrous oxide fluxes following bovine urine deposition to summer-grazed pasture. *New Zealand J. Agri. Res.* **57**, 136–147 (2014).
- Ma, L., Shan, J. & Yan, X. Nitrite behavior accounts for the nitrous oxide peaks following fertilization in a fluvo-aquic soil. *Biol. Fert. Soils.* doi: 10.1007/s00374-015-1001-8 (2015).
- Van Cleemput, O. & Samatar, A. H. Nitrite in soils: accumulation and role in the formation of gaseous N compounds. *Fert. Res.* **45**, 81–89 (1996).
- Anthonisen, A. C., Loehr, R. C., Prakasam, T. B. S. & Srinath, E. G. Inhibition of nitrification by ammonia and nitrous acid. *J. Water Poll. Control Fed.* **48**, 835–852 (1976).
- Park, S. & Bae, W. Modeling kinetics of ammonium oxidation and nitrite oxidation under simultaneous inhibition by free ammonia and free nitrous acid. *Process Biochem.* **44**, 631–640 (2009).
- Jiang, X., Ma, Y., Yuan, J., Wright, A. L. & Li, H. Soil particle surface electrochemical property effects on abundance of ammonia-oxidizing bacteria and ammonia-oxidizing archaea, NH₄⁺ activity, and net nitrification in an acid soil. *Soil Biol. Biochem.* **43**, 2215–2221 (2011).
- Wang, B., Zhao, J., Guo, Z., Ma, J., Xu, H. & Jia, Z. Differential contributions of ammonia oxidizers and nitrite oxidizers to nitrification in four paddy soils. *ISME J.* doi: 10.1038/ismej.2014.194 (2014).
- Ke, X., Angel, R., Lu, Y. & Conrad, R. Niche differentiation of ammonia oxidizers and nitrite oxidizers in rice paddy soil. *Environ. Microbiol.* **15**, 2275–2292 (2013).
- Ollivier J. *et al.* Effects of repeated application of sulfadiazine-contaminated pig manure on the abundance and diversity of ammonia and nitrite oxidizers in the root-rhizosphere complex of pasture plants under field conditions. *Front. Microbiol.* **4**, 22 (2013).
- Wrage N., Velthof, G. L., van Beusichem, M. L. & Oenema, O. Role of nitrifier denitrification in the production of nitrous oxide. *Soil Biol Biochem.* **33**, 1723–1732 (2001).
- Venterea, R. T. Nitrite-driven nitrous oxide production under aerobic soil conditions: Kinetics and biochemical controls. *Global Change Biol.* **13**, 1798–1809 (2007).
- McBride, M. in *Environmental chemistry of soils*, Ch. 3, 63–120 (Oxford University Press, 1994).

22. Kissel, D. E., Cabrera, M. L. & Paramasivam, S. Ammonium, ammonia, and urea reactions in Soils in *Nitrogen in agricultural systems*, (eds Schepers, J. S. & Raun, W. R.) Ch. 4, 101–155 (American Society of Agronomy, 2008).
23. Sumner, M. Measurement of soil pH: Problems and solutions. *Commun. Soil Sci. Plan.* **25**, 859–879 (1994).
24. Venterea, R. T. & Rolston, D. Nitric and nitrous oxide emissions following fertilizer application to agricultural soil: Biotic and abiotic mechanisms and kinetics. *J. Geophys. Res-Atm.* **105**, 15117–15129 (2000).
25. Stevenson, F., Harrison, R., Wetselaar, R. & Leeper, R. Nitrosation of soil organic matter: II. Nature of gases produced by reaction of nitrite with lignins, humic substances and phenolic constituents under neutral and slightly acidic conditions. *Soil Sci. Soc. Amer. Proc.* **34**, 430–435 (1970).
26. Minami, K. & Fukushi, S. Emission of nitrous oxide from a well-aerated Andosol treated with nitrite and hydroxylamine. *Soil Sci. Plant Nutr.* **32**, 233–237 (1986).
27. Venterea, R. T. & Rolston, D. E. Mechanisms and kinetics of nitric and nitrous oxide production during nitrification in agricultural soil. *Global Change Biol.* **6**, 303–316 (2000).
28. Huang, T. *et al.* Ammonia-oxidation as an engine to generate nitrous oxide in an intensively managed calcareous Fluvo-aquic soil. *Sci. Reports.* **4**, 3950 doi: 10.1038/srep03950 (2015).
29. Zhu, X., Burger, M., Doane, T. A. & Howarth, W. R. Ammonia oxidation pathways and nitrifier denitrification are significant sources of N₂O and NO under low oxygen availability. *P. Natl. Acad. Sci. USA* **110**, 6328–6333 (2013).
30. Goreau, T. J. *et al.* Production of NO₂⁻ and N₂O by nitrifying bacteria at reduced concentrations of oxygen. *Appl. Environ. Microbiol.* **40**, 526–32 (1980).
31. Whitehead, D. C., Lockyer, D. R. & Raistrick, N. Volatilization of ammonia from urea applied to soil: Influence of hippuric acid and other constituents of livestock urine. *Soil Biol. Biochem.* **21**, 803–808 (1989).
32. Spott, O., Russow, R. & Stange, C. F. Formation of hybrid N₂O and hybrid N₂ due to codenitrification: First review of a barely considered process of microbially mediated N-nitrosation. *Soil Biol Biochem.* **43**, 1995–2011 (2011).
33. Suzuki, I., Dular, U. & Kwok, S. C. 1974. Ammonia or ammonium ion as substrate for oxidation by *Nitrosomonas europaea* cells and extracts. *J. Bacteriol.* **120**, 556–558 (1974).
34. Monaghan, R. M. & Barraclough, D. Some chemical and physical factors affecting the rate and dynamics of nitrification in urine-affected soil. *Plant Soil.* **143**, 11–18 (1992).
35. Di, H. J., Cameron, K. C., Shen, J. P., Winefield, C. S., O'Callaghan, M. S. B. & He, J. Z. Nitrification driven by bacteria and not archaea in nitrogen-rich grassland soils. *Nat. Geoscience.* **2**, 621–624 (2009).
36. Gubry-Rangin, C., Nicol, G. W. & Prosser, J. I. Archaea rather than bacteria control nitrification in two agricultural acidic soils. *FEMS Microbiol. Ecol.* **74**, 566–574 (2010).
37. Zhao, W. *et al.* Adsorption and desorption characteristics of ammonium in eight loams irrigated with reclaimed wastewater from intensive hogpen. *Environ. Earth Sci.* **69**, 41–49 (2013).
38. Mulvaney, R. L. Nitrogen-Inorganic forms in *Methods of soil analysis Part 3-Chemical Methods*, (ed. Sparks, D. L.) Ch. 38, 1123–1184 (American Society of Agronomy, 1996).
39. Vogeler, I., Cichota, R., Snow, V. O., Dutton, T. & Daly, B. Pedotransfer functions for estimating ammonium adsorption in soils. *Soil Sci. Soc. Am. J.* **75**, 324–331 (2011).
40. Bates, R. G. & Pinching, G. D. Acidic dissociation constant of ammonium ion at 0° to 500° C and the base strength of ammonia. Res. Paper RP1982. J. Res. Natl. Bur. Standards. U.S. Dep. Commerce, Natl. Bureau Standards. **42**, 419–430 (1949).
41. Clough, T. J., Kelliher, F. M., Wang, Y. P. & Sherlock, R. R. Diffusion of ¹⁵N-labelled N₂O into soil columns: a promising method to examine fate of N₂O in subsoils. *Soil Biol. Biochem.* **38**, 1462–1468 (2006).
42. Stevens, R. & Laughlin, R. Nitrite transformations during soil extraction with potassium chloride. *Soil Sci. Soc. Am. J.* **59**, 933–938 (1995).
43. Caporaso, J. G. *et al.* Ultra-high-throughput microbial community analysis on the Illumina HiSeq and MiSeq platforms. *ISME J.* **6**, 1621–1624 (2012).
44. Francis, C. A., Roberts, K. J., Beman, J. M., Santoro, A. E. & Oakley, B. B. Ubiquity and diversity of ammonia-oxidizing archaea in water columns and sediments of the ocean. *P. Natl. Acad. Sci. USA* **102**, 14683–14688 (2005).
45. Rothauwe, J. H., Witzel, K. P. & Liesack, W. The ammonia monooxygenase structural gene amoA as a functional marker: Molecular fine-scale analysis of natural ammonia-oxidizing populations. *Appl. Environ. Microbiol.* **63**, 4704–4712 (1997).
46. Wertz, S., Poly, F., Le Roux, X. & Degrange, V. Development and application of a PCR-denaturing gradient gel electrophoresis tool to study the diversity of *Nitrobacter*-like nxrA sequences in soil. *FEMS Microbiol. Ecol.* **63**, 261 (2008).
47. Caffrey, J. M., Bano, N., Kalanetra, K. & Hollibaugh, J. T. Ammonia oxidation and ammonia-oxidizing bacteria and archaea from estuaries with differing histories of hypoxia. *ISME J.* **1**, 660–662 (2007).
48. Burton, D. L., Li, X. & Grant, C. A. Influence of fertilizer nitrogen source and management practice on N₂O emissions from two Black Chernozemic soils. *Can. J. Soil Sci.* **88**, 219–227 (2008).

Acknowledgments

The authors gratefully acknowledge the assistance of S. Mitchell, P. Wang and M. Sadowsky in establishing the PCR methods, and S. Khan, S. Mitchell, K. Sidla and M. Dolan in assisting with laboratory analysis. This work was supported by a Global Research Alliance Senior Scientist (GRASS) fellowship to R. Venterea and T. Clough from the Livestock Emissions and Abatement Research Network.

Author Contributions

RV and TC designed and conducted the experiments. RV developed the equations, performed data reduction, prepared the figures and wrote the manuscript. JC performed the statistical analyses. PW, MS and FB-S developed the qPCR methods. FB-S conducted the qPCR analyses. TC, JC and FB-S revised and wrote specific sections of the manuscript.

Additional Information

Supplementary information accompanies this paper at <http://www.nature.com/srep>

Competing financial interests: The authors declare no competing financial interests.

How to cite this article: Venterea, R. T. *et al.* Ammonium sorption and ammonia inhibition of nitrite-oxidizing bacteria explain contrasting soil N₂O production. *Sci. Rep.* **5**, 12153; doi: 10.1038/srep12153 (2015).



This work is licensed under a Creative Commons Attribution 4.0 International License. The images or other third party material in this article are included in the article's Creative Commons license, unless indicated otherwise in the credit line; if the material is not included under the Creative Commons license, users will need to obtain permission from the license holder to reproduce the material. To view a copy of this license, visit <http://creativecommons.org/licenses/by/4.0/>

SCIENTIFIC REPORTS

OPEN

Corrigendum: Ammonium sorption and ammonia inhibition of nitrite-oxidizing bacteria explain contrasting soil N₂O production

Rodney T. Venterea, Timothy J. Clough, Jeffrey A. Coulter, Florence Breuillin-Sessoms, Ping Wang & Michael J. Sadowsky

Scientific Reports 5:12153; doi: 10.1038/srep12153; published online 16 July 2015; updated on 08 February 2016

Ping Wang and Michael J. Sadowsky were omitted from the author list in the original version of this Article. This has been corrected in the PDF and HTML versions of the Article.

The Author Contributions section now reads:

“RV and TC designed and conducted the experiments. RV developed the equations, performed data reduction, prepared the figures and wrote the manuscript. JC performed the statistical analyses. PW, MS and FB-S developed the qPCR methods. FB-S conducted the qPCR analyses. TC, JC and FB-S revised and wrote specific sections of the manuscript.”



This work is licensed under a Creative Commons Attribution 4.0 International License. The images or other third party material in this article are included in the article's Creative Commons license, unless indicated otherwise in the credit line; if the material is not included under the Creative Commons license, users will need to obtain permission from the license holder to reproduce the material. To view a copy of this license, visit <http://creativecommons.org/licenses/by/4.0/>